EDITOR'S CHOICE

EXPERIMENTS OF UNDERWATER SPARK DISCHARGES WITH PINCHED ELECTRODES

Takaaki Matsumoto [1]

ABSTRACT

Experiments of sparking discharges were performed in ordinary water mixed with potassium carbonate. Here thin metal wires of palladium, nickel, titanium, iron, cadmium, molybdenum and tungsten were used as electrodes. In high voltages over 40 V, the surface of the electrode was pinched so that sparking appeared on the cathode or anode, and simultaneously extraordinary phenomena were observed. Especially, microscopic ring-clusters generated on the cathode caused tiny ball-lightning-like phenomena. The extraordinary phenomena was explained by The Nattoh Model.

INTRODUCTION

Recently many experiments of the electrolysis of heavy water have been performed since the cold fusion phenomena was published [1]. The studies have been mainly focussed to reproduce and enhance the excess heat, in which deuterium is charged into a metal to induce the cold fusion reactions. On the other hand, the author earlier proposed The Nattoh Model predicting that the cold fusion reactions can be induced in an extremely compressed hydrogen-cluster ("itonic" state) that can be easily generated by an electrical discharge [2], and showed that many extraordinary phenomena appeared associated with the cold fusion reactions in the experiments of the pulsed electrical discharge in water [3, 4].

This paper describes experiments of continuous discharges in ordinary water mixed with potassium carbonate, in which thin metal wires were used. Here the pinch effect of the current effectively worked to compress hydrogen-clusters on the cathode so that sparking appeared, associated with many extraordinary phenomena. Especially, many microscopic ring-clusters generated on the cathode caused tiny ball-lightning-like phenomena. The extraordinary phenomena were explained by The Nattoh Model.

EXPERIMENT

Experiments of the sparking discharge were performed using the DC continuous discharge in ordinary water. The experimental arrangement is shown in Fig. 1.

Thin wires of pure metals of palladium (99.95 %, 0.50 mm ϕ), nickel (99.7 %, 0.50 mm ϕ), titanium (99.9%, 1.0 mm ϕ), iron (99.998 %, 1.0 mm ϕ), cadmium (99.9999 %, 1.0

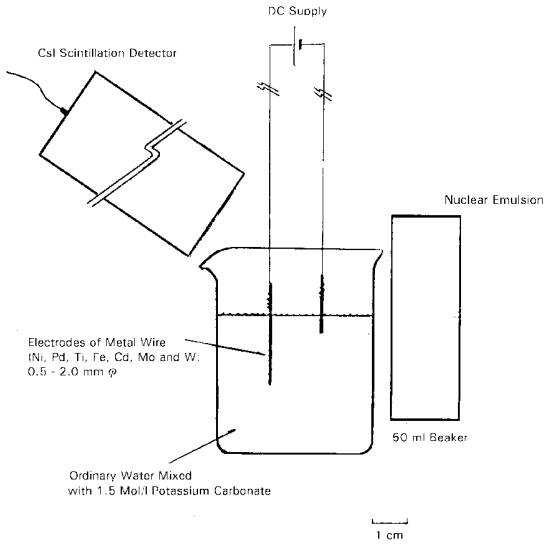

Fig. 1

[1] Dept. of Nuclear Engineering, Hokkaido Univ., Sapporo, 060 Japan

mm ϕ), molybdenum (99.95 %, 1.0 mm ϕ) and tungsten (99.95 %, 2.0 mm ϕ) were used as the electrodes. The wire electrodes were vertically immersed in ordinary water mixed with about 1.5 mol../l potassium carbonate, that was contained in a glass beaker (45 mm ϕ). The effective lengths of the cathode and anode that were inserted in the solution were about 3 mm and 15 mm long, respectively. On the shorter electrode, the current density could be increased such that the pinch effect of the current effectively worked to compress hydrogen molecules [2].

The DC discharge was continuously employed between the electrodes, in which the voltage was varied up to about 150 V under the constant voltage mode. The sparking that appeared on the surface of the electrode over 40 V was observed by a system of a micro telescope and a video tape recorder (VTR). The emission of radiation was monitored by a spectroscopy with a CsI(Tl) scintillation detector (12.5 mm x 12.5 mm x 20.0 mm). Furthermore, nuclear emulsions were located near the cathode. The nuclear emulsions (100 μm x 50 mm x 50 mm, coated on both sides of 1 mm thick acrylic plate) were the same as those that were used in previous experiments [5, 6]. After the discharges, the electrodes were analyzed by an optical microscope (OM), a scanning electron microscope (SEM) with an energy dispersive X-ray spectroscopy (EDX), an electron probe microscope analyzer (EPMA) and a X-ray spectroscopy (XS).

RESULTS

A. Nonlinear Characteristics of I/V

The DC current was employed between the electrodes under the constant voltage mode. Fig. 2 shows the strong nonlinearity of the I/V characteristics in which the nickel wires were used for both the electrodes and the cathode was shorter. They were divided into three regions. In the lower voltage region, about 40 V, the current proportionally increased as the voltage increased. Here, the layer of the resolved hydrogen gas also was steadily increased on the cathode. In the intermediate voltage region between about 40 V and 60 V, the hydrogen gas seemed to burst and evolve from the cathode, and the current strongly fluctuated. In the higher voltage region, about 60 V, the pinch effect of the current effectively worked to suppress the gas evolution, and tiny sparks appeared on the surface of the cathode. They initially appeared on the bottom tip of the cathode and as the voltage increased, the number of the tiny sparks increased to eventually cover the whole surface of the cathode. Here, the current was strongly suppressed to a stable level of about 0.1 A.

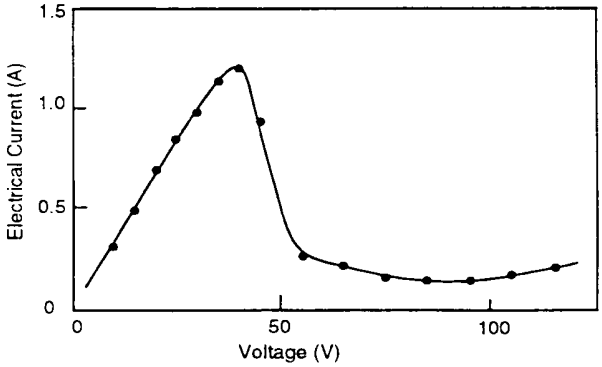

Fig. 2 Nonlinear I/V Curve

The I/V curve somewhat depended on the condition of the electrodes. Fig. 2 was obtained with new nickel electrodes. With old electrodes, impurity deposits on the surface, such as the electrolyte of potassium somewhat changed the I/V curve. However, the general aspect of the I/V curve showing three divided regions was maintained throughout the experiments.

B. VTR Observation of Microsparks

How the tiny sparks appeared depended on the kinds of electrode materials. Titanium was special among the metals used in these experiments. When the same metal wires were used for both of the electrodes, the tiny sparks appeared only on the anode of titanium, while with all the other metals, they initially appeared on the cathode and sequentially on the anode in the high voltage. With all the metals except titanium, it was also possible to generate the tiny sparks on the anode, but in that case, platinum was used as the cathode and simultaneously the voltage was required to increase higher than about 150 V. We made the tiny sparks appear on the cathode even with titanium, but the other metals, such as platinum, were used as the anode. This

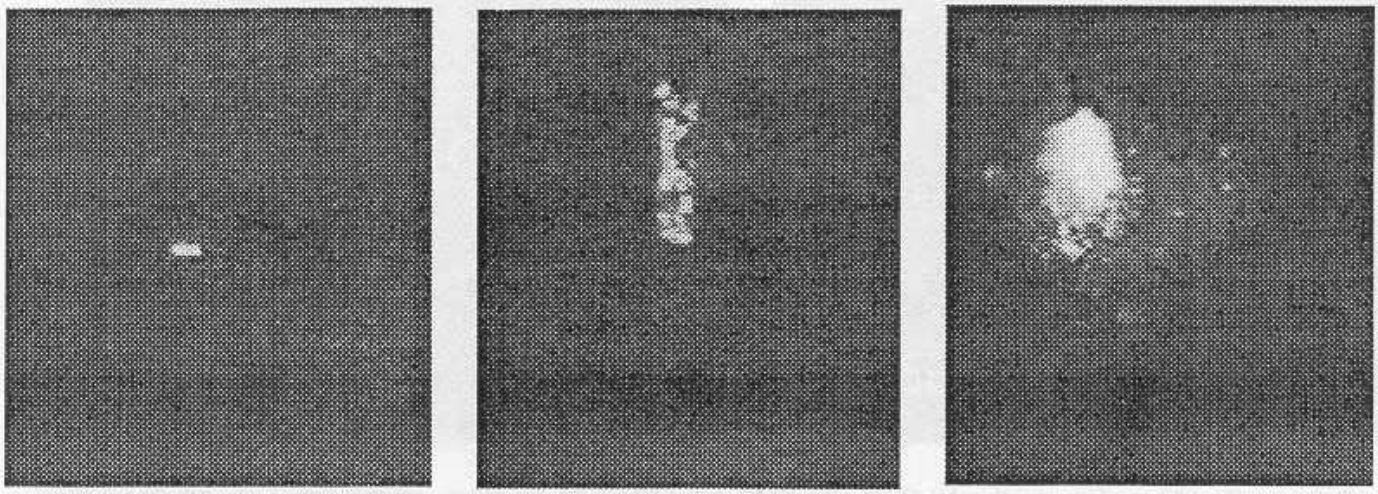

Fig. 3 Tiny sparks on the Palladium Cathode (x 10)
a) about 45 V, b) about 60 V, c) about 70 V.

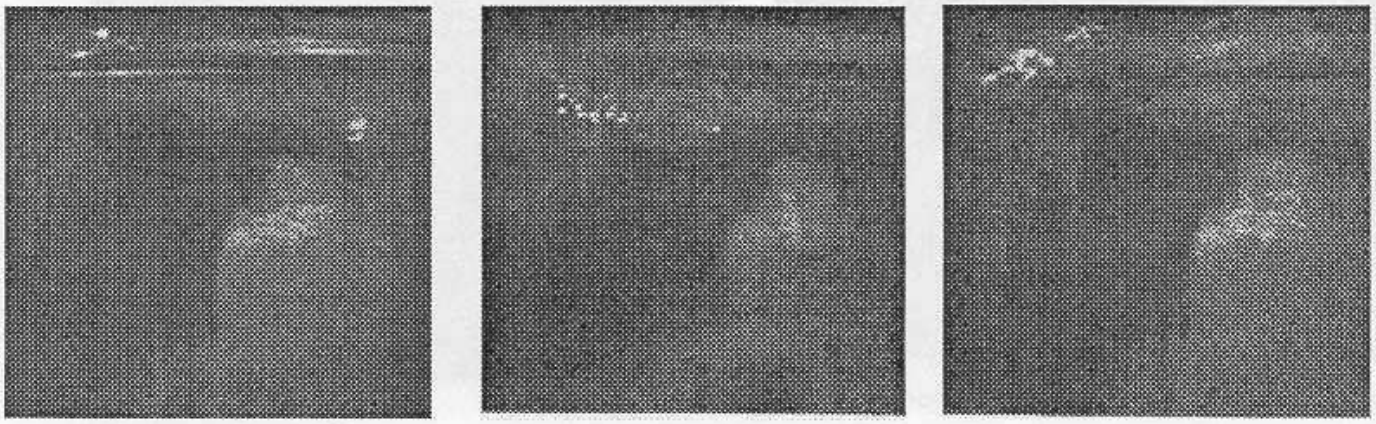

Fig. 4 Separated Tiny Sparks (time step 33 msec)

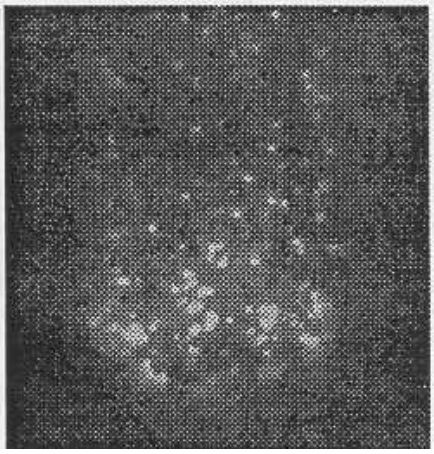

Fig. 5
Microsparks on the Cadmium Cathode
(x 200)

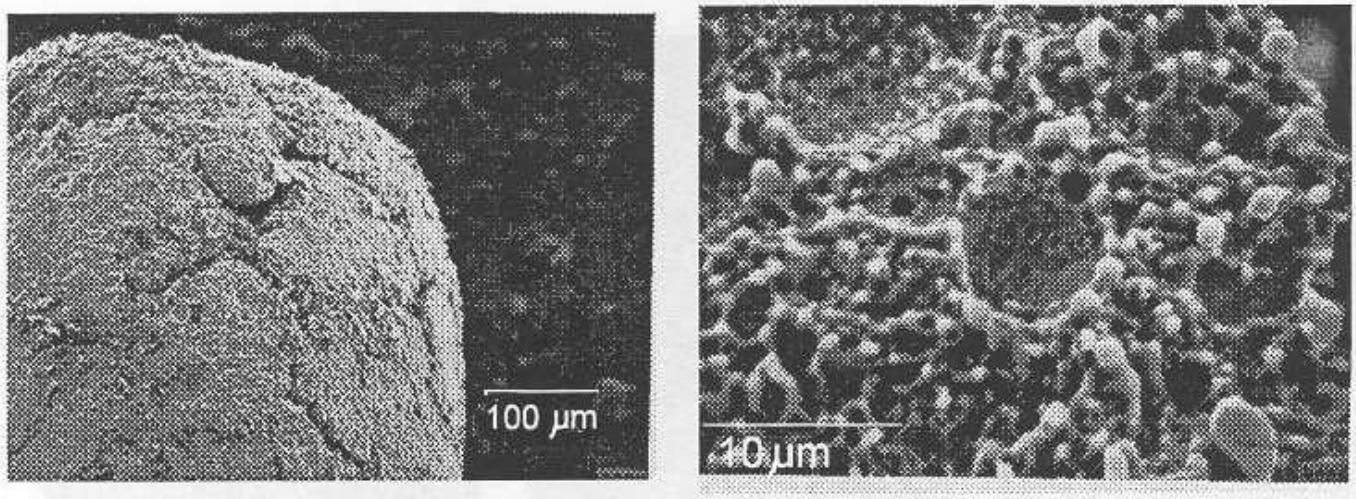

Fig. 7 Deposited Materials on the Ni Cathode (left) deposits with fracture, (right) tiny hole on deposits

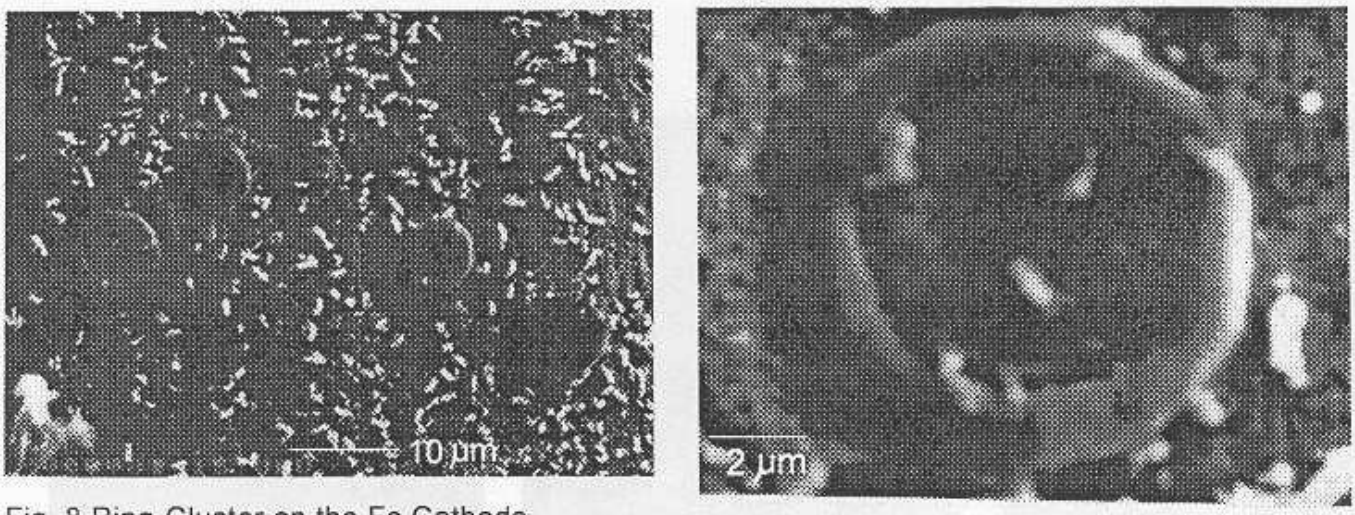

Fig. 8 Ring-Cluster on the Fe Cathode

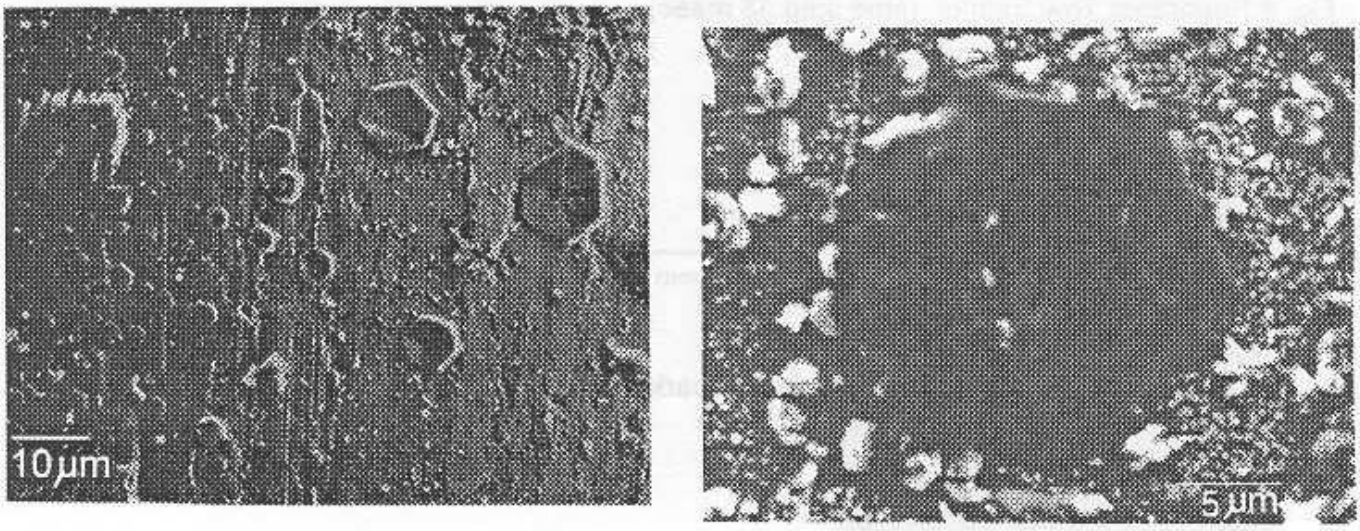

Fig. 9 Hexagonal Decay Products: (left) hexagonal plates, (right) intermediate stage of decay.

suggested that there might be different processes for sparking on the cathode or anode, and with titanium or the other metals.

The tiny sparks were observed *in situ* using the VTR system. Fig. 3 shows the tiny sparks appearing on the surface of the nickel wire cathode (with 10 times amplification of the VTR monitor). Figs. 3(b) and 3© show that the number of the tiny sparks increased as the voltage increased, but no sparks appeared on the anode.

Fig. 4 shows a sequence of pictures for the tiny sparks, in which they were accidentally separated from the surface of the palladium cathode by two explosions. The first small explosion took place in the gas atmosphere over the water level, which was triggered by the tiny sparks, as shown in Fig. 4(a). Due to mechanical shock from the explosion, a group of the tiny sparks were separated from the cathode, and were driven by the electrical potential towards the anode, as is shown in Fig. 4(b). The tiny sparks were decayed on the anode to trigger the second explosion, as shown in Fig. 4(c). These pictures showed that the tiny sparks were negatively charged and could exist in water solution as independent bodies.

The tiny sparks were observed in more detail using the VTR system with amplification of 200 times. Fig. 5 shows the expanded pictures of the tiny sparks appearing on the cadmium cathode. The tiny sparks were found to consist of a large number of microsparks, that were frequently created or broken. The microsparks sometimes formed ring-clusters with a diameter of about 100 μm and decayed to something like a black cloud that prevented the backside light from shining through. Furthermore, there were bright spots among the microsparks. A corona-like discharge was observed from the bright spot. The decay of the microsparks will be examined in more detail.

C. Emission of Radiation

The emission of radiations was monitored by the CsI(T1) scintillation spectroscopy. Certain kinds of radiation were observed to be released through the wall of the glass beaker.

The CsI(T1) scintillation detector was alternatively placed outside the glass beaker and over the water surface. The detector measured the emission of radiation in the high voltages in both cases. The energy spectrum of the radiations were continuous and monotonously declined as the energy increased. The typical spectra are shown in Fig. 6. The background was measured with no discharges. The counting rate was significantly higher than the background. As the voltage increased, the energy tail expanded more widely. The intensity of the radiation sharply dropped as the distance between the detector and the cathode increased. The radiation detected was neither gamma rays nor X-rays. The signals were generated by electromagnetic waves picked up with the electrical circuit. The emission of the electromagnetic waves will be discussed relating to the break-up of the ironic clusters.

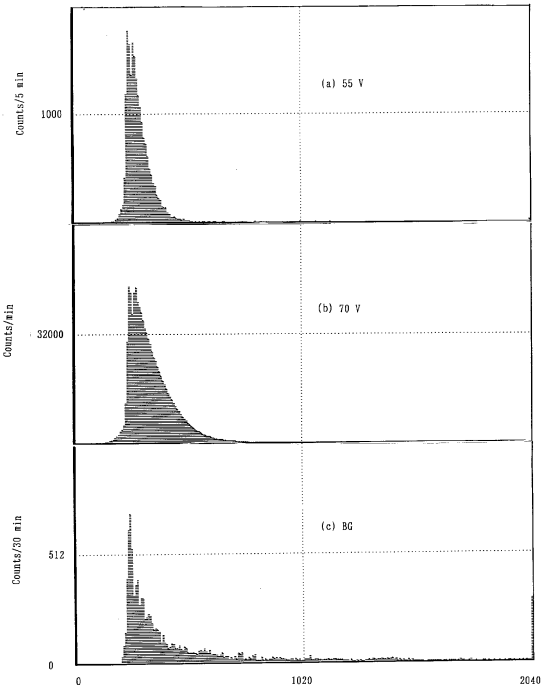

Fig. 6

D. Nuclear Transmutation

Discharge products deposited on the electrode surface were examined by SEM-EDX, EPMA and XS. Several kinds of the nuclear transmutation occurred.

Fig. 7 shows a SEM picture of the deposited materials on the cathode of the nickel wire. Thick layers including potassium were deposited **and there were many tiny holes (about 10 μmϕ)** over which the microsparks might be shining through [emphasis by Ed.].

Several elements were found by EPMA among the deposited materials on the anode of palladium wire: nickel, calcium, titanium, sodium, aluminum, chlorine, cadmium and iodine. They were not observed in a reference region of the palladium wire. Furthermore, nickel was clearly detected by XS. These elements could not be assigned to impurities but rather suggested to be transmuted during the electrical discharges associated with the microsparks. For example, chlorine, calcium and nickel could be transmuted by the capture of electrons, a proton and hydroxide with a potassium nucleus, respectively. On the other hand, cadmium and iodine could be transmuted by the capture of a proton and oxygen with a palladium nucleus, respectively. Such captures could occur in the highly compressed state of the hydrogen-cluster.

E. Microscopic Ring-Clusters

When the iron wires were used for the electrodes, tiny ring products were successfully caught on the surface of the cathode. The discharge was maintained with 70 V and 0.3 A for 27 min. and in the last period, there was a small explosion.

Many ring products could be observed with SEM around the zone on the surface of the cathode that touched the water level, as shown in Fig. 8. Simultaneously regular hexagonal products were observed in the same zone, as shown in Fig. 9. After a few days, the ring products all disappeared, and in place of them, only the hexagonal products remained. This suggests that the ring products decayed to the hexagonal plates. Fig. 9(b) shows the intermediate stage of the decay in which an inner circular zone still remained.

The ring and the hexagonal products were examined with EPMA. Fig. 10 shows dimensional distributions of the elements that were found near the products. Besides iron from the host metal and potassium from the electrolyte, some elements of calcium, sodium, chlorine and cadmium were both observed in the ring and the hexagonal products. Two circular zones, especially, could be seen for cadmium that were clearly separated from each other in the ring products, as shown in Fig. 10. Those observations suggest that the ring product could consist of a hydrogen-cluster and that the process of the nuclear transmutation took place in the clusters.

F. Nuclear Emulsions

Five plates of nuclear emulsions were placed to monitor particles that were emitted during the electrical discharges. Fig. 11 shows extraordinary rail-like traces observed on the surface of the first nuclear emulsion. Similar traces were not found in the other nuclear emulsions. Reference nuclear emulsions were located at 5 m distance from the cell in the same room, but similar traces were found neither in nor on the reference nuclear emulsions. The traces suggested that some particles walked around on the surface. Fig. 11(b) shows a ring product left with the rail-like trace. This clearly indicates that the extraordinary rail-like traces were generated by the ring products that escaped from the cell and walked around on the surface of the first nuclear emulsion. The diameter of the ring was about 10 μm, which was approximately the same as that of the ring products observed on the iron electrode. This observation suggests an extraordinary result that the ring product could penetrate through the glass wall of the beaker and the water solution. The curious behaviors of the ring product will be further discussed in Sec. 4.

G. Miscellaneous

The other extraordinary phenomena were observed during or after the discharge experiments.

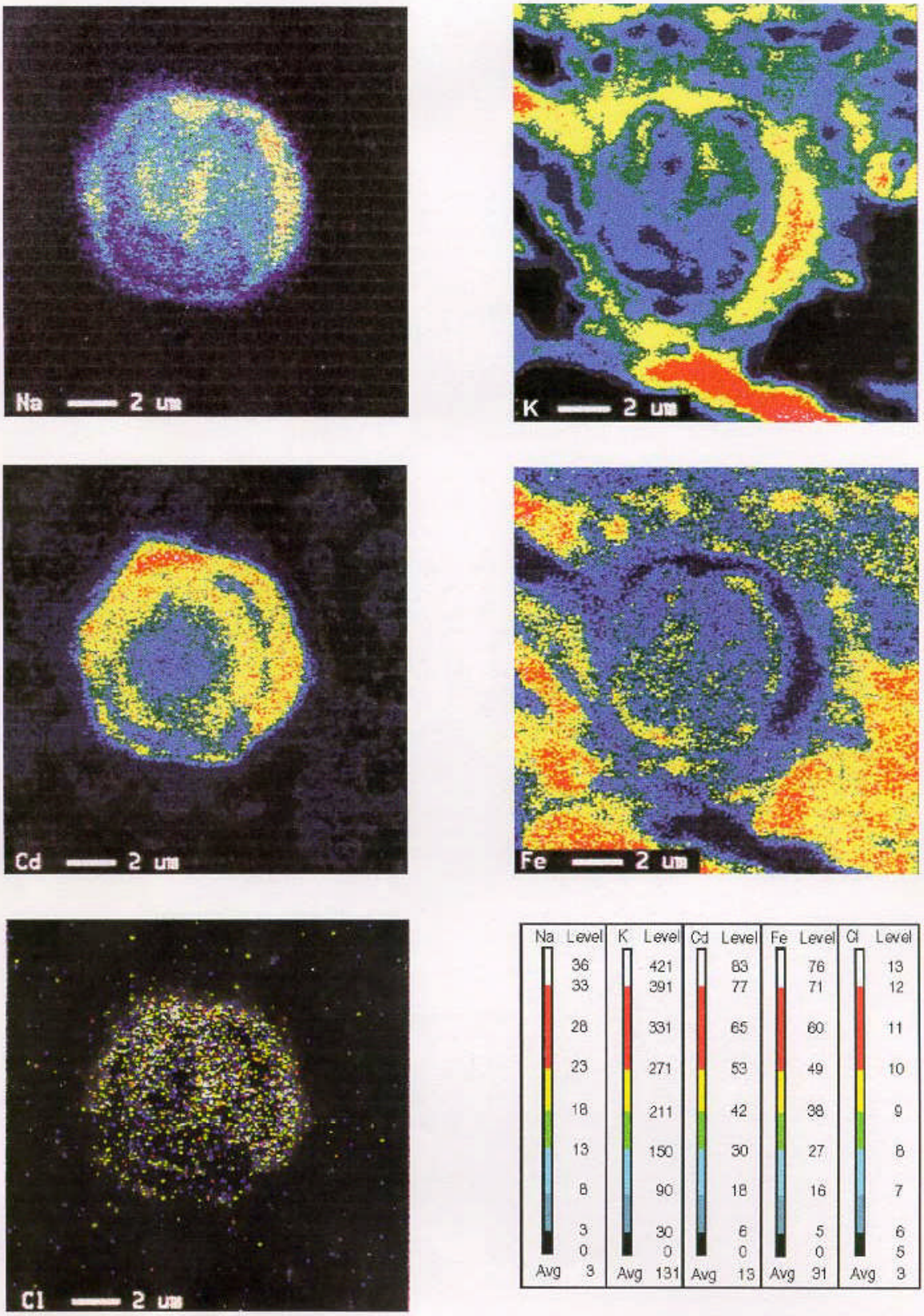

Fig. 10 EPMA Analysis of the Hexagonal Decay Product

BLANK

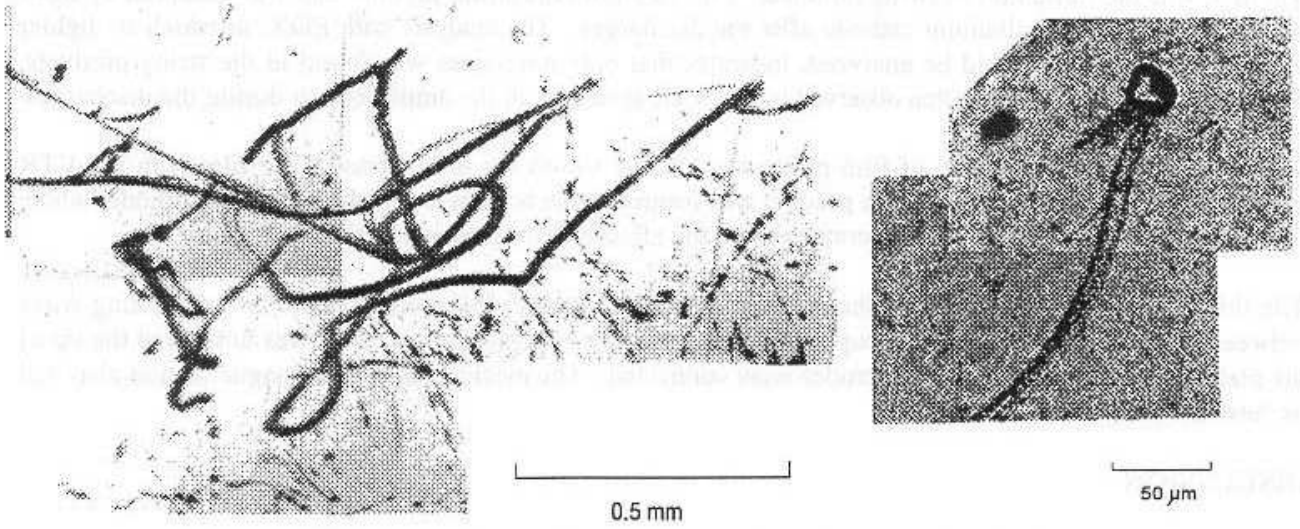

Fig. 11 Rail-like Traces: a) trace-like written with one stroke; b) trace with ring-like product.

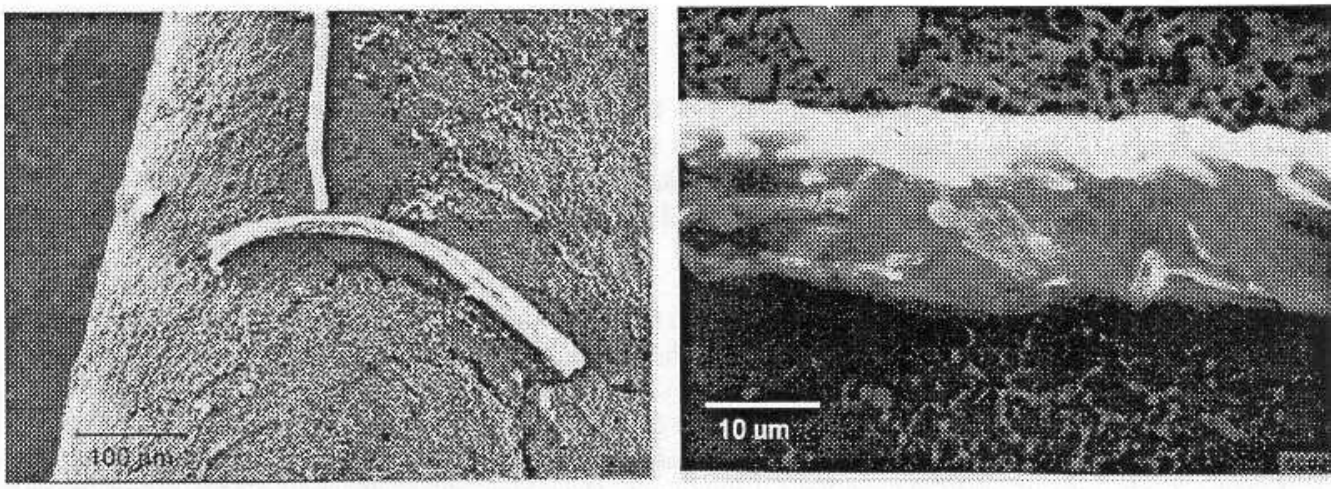

Fig. 12 String Product on the Pd Cathode

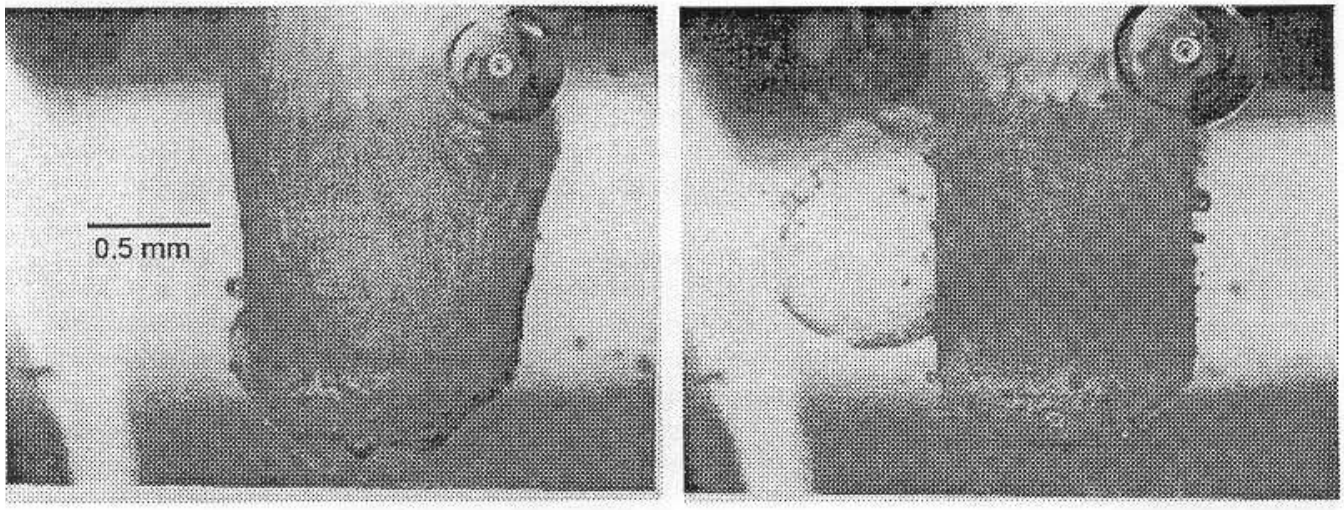

Fig. 13 Film Product on the Cd Cathode

The first was the formation of string products. Fig. 12 shows the string product that was observed by SEM on the surface of the palladium cathode after the discharges. The analysis with EDX, in which no lighter elements than sodium could be analyzed, indicates that only potassium was found in the string products. Similar string products were often observed by the VTR system with the amplification during the discharges.

The second was the formation of film products. Fig. 13 shows the production of the film with the VTR system (100 amplification). The film product was formed at the bottom top of the cadmium cathode, where the microsparks were frequently generated due to the effective compression of the hydrogens.

The third was the magnetization of the platinum wires (0.5 mm ϕ) that were used for the connecting wires between the wire electrode and the copper leading wire. The magnetization effect was noticed at the tip of the platinum wires, at which the electrodes were connected. The mechanisms of the magnetization also will be further discussed.

DISCUSSION

Many extraordinary phenomena were observed during the sparking underwater discharges. The mechanisms of some important phenomena are discussed here.

A. Formation of Microsparks

The first phenomena is concerned with the tiny sparks. The appearance of the tiny sparks somewhat depends on the kinds of the electrode materials. Titanium was special among the metals used in these experiments. With metals such as palladium and nickel, the tiny sparks initially appeared on the surface of the cathode, and as the voltage increased, they also appeared on the anode. These facts suggest that there were two processes for the formation of the tiny sparks.

On the pinched cathode, hydrogens were compressed to the high concentration on the surface of the electrode by the electrical potential, and simultaneously the high current density of the electrons were charged so that the itonic state of the hydrogen-clusters was formed [2]. The itonic hydrogen-clusters could emit the visible light from the microsparks because the itonic mesh was excited by the nuclear fusion reactions. On the other hand, on the anode, the hydroxyl radicals were compressed by the electrical potential. The itonic state of the hydroxyl radicals were also formed to emit the visible light. Here, since the heavy atoms of the oxygen were included, the higher voltage was required to generate the microsparks than on the cathode.

In the intermediate voltage region between about 40 V and 60 V, where the voltage was critical to the formation of the itonic hydrogen-clusters, the resulted clusters would sometimes break up. This was a reason why the rapid evolution of the hydrogen gas seemed to occur on the cathode. On the contrary, the current was strongly suppressed by the appearance of the microsparks in the high voltage region. This was because the itonic hydrogen-clusters, negatively charged, covered the cathode to prevent the free flow of the current. Furthermore, the break up of the microsparks caused the spatial charge effects to reduce the current.

With titanium, different processes were suggested for the generation of the microsparks, that appeared on the anode in the low voltage region. The microsparks on the titanium anode were examined in a previous experiment of the AC discharges [7]. Here the microsparks appeared when the deposited materials were taken away and the local, but rapid, electrical discharges occurred. Fig. 14 shows a picture of the microspark products that were caught by a copper plate placed near the titanium electrode over the water level. The figure showed that the microspark products had the mesh structure. This means that the deposited materials were in the itonic state. Furthermore, inside the meshes, there were observed bright spots suggesting some nuclear reactions.

B. Extraordinary Ring-Cluster

The second concerns with the ring-cluster. It could easily penetrate materials like glass and eventually decayed to the almost hexagonal plates. There are two candidate models for mechanisms of forming the ring-cluster.

The first is the hydrogen ring-cluster with the closed current. When the compression of the hydrogen-cluster was proceeded on the pinched electrode in the high voltage region, some phase transition might have occurred in the hydrogen-clusters, because the hydrogens had no places to escape. The compression of the hydrogens was made two dimensionally on the surface of the pinched cathode so that the ring could have the minimum total energy. In the ring-cluster, closed electrical current could flow and it induced the magnetization effect. The ring-clusters could be negatively charged.

The second is a special kind of product represented by tiny white holes. The tiny white hole was early observed by the author in a previous Mills's- type experiment of electrolysis with light water and a nickel electrode [2]. There a lot of conic [sic] products were observed as evolved products resulted in the tiny white holes. In this experiment, especially with cadmium, the collapsed mass should be heavy so that evolved products might be curled up to form the ring structure.

It is remarkable to note that the ring-clusters could penetrate the regions such as glass, walk around on the surface of the nuclear emulsions and hop up and down between the nuclear emulsions [4]. These phenomena could be explained by charges associated with the ring-clusters. When the ring-cluster touched the material, a portion of the charges of the ring-cluster transferred to the material, and the repulsive force was generated between the ring-cluster and the material. This force could make the ring-cluster jump-up. When the ring-cluster penetrated through the material, the constituent atoms of the material could be sequentially absorbed into the ring-cluster. Then a microscopic hole having the similar diameter could be left in the solid state material.

However, the curious penetration of the ring-cluster cannot be explained by the first model. On the other hand, the second model seems to easily explain the penetration, because a tiny white hole is produced from a tiny black hole that should have the extremely small dimension compared with interatomic distance. Here the hexagonal plate generated from the decay of the ring-cluster should be explained as the crystallization of compressed materials included in the ring-cluster.

The magnetization effect was observed on the tip of the leading wires of platinum that were connected with the electrodes. The effect could be explained by the existence of the tiny magnets, i.e., the ring-clusters. Furthermore, when the decay proceeded further, corona-like discharge phenomena could be induced at the center of the ring-cluster, as observed *in situ* by the VTR system. Here the break-up of the ring-clusters could make the electromagnetic waves emit, as were detected by the CsI(Tl) scintillation detector. Similar radiation could also be emitted by the break-up of the itonic hydrogen-clusters.

The extraordinary behavior of the ring-clusters were very similar to those reported about the curious natural phenomena, ball-lightning [8, 9]. Ball-lightning is often born associated with a thunderstorm, that is, the electrical discharges on the large scale. It is reasonable to consider that during the thunderstorm, some products like the ring-cluster obtained in this experiment might be generated, move around and eventually explode, as were reported in the references [8, 9].

C. Nuclear Transmutation

The nuclear transmutation took place during the underwater spark discharges. The nuclear transmutation can take place in the itonic hydrogen-clusters, explained in Ref. [2]. Here, the hydrogens were so highly

compressed that various kinds of the nuclear transmutation became possible. The feasible schemes of the nuclear transmutation are described in an appendix for the case of the iron electrodes and the potassium electrolyte.

Furthermore, the analysis with EPMA showed that the nuclear transmutation was possible in the ring-cluster. This fact suggests that there might be another process for the nuclear transmutation, different from the nuclear transmutation in the itonic hydrogen-clusters. The ring-cluster showing the crystallization effect should have higher concentration of the atoms than the solid state. This makes the nuclear transmutation possible. In the appendix, the production of the cadmium element is explained by the fusion reaction between two iron nuclei.

CONCLUSIONS

In the experiments of the underwater discharges, the microsparks on the pinched electrodes were examined in detail. It was found that they were not normal sparks but consisted of the itonic hydrogen-clusters that were sometimes transformed to the ring-clusters. The itonic hydrogen-cluster and the ring-cluster could exist for a moment as an independent body. The ring-cluster can easily penetrate through the layers of glass or acrylic despite their heavy mass and charges, and hop up and down on the nonconductive materials such as nuclear emulsions. It is remarkable that the nuclear transmutation caused by the nuclear fusion reactions took place in the ring-cluster as well as in the itonic hydrogen-cluster. The ring-cluster was very similar to ball-lightning that was observed in the natural environment, although the scale was different. As the current density or voltage were increased, the ring-cluster with the larger dimension could even be produced in laboratory. The reproducibility of the underwater spark discharges method is so good that the property of ball-lightning should be examined in detail in laboratory.

Acknowledgments

The author is thankful to Mrs. N. Miyazaki and T. Suda for their help during the observation with the microscopies.

REFERENCES

1. See the proceedings of the International Cold Fusion Conference from 1 to 6, or related papers published in *Fusion Technology* in 1989 - 1996.
2. T. Matsumoto, "Mechanisms of Cold Fusion: Comprehensive Explanations by The Nattoh Model,"*Memoirs of the Faculty of Engineering*, Hokkaido Univ., vol 19, no 2, p 201- 224 (1995).
3. T. Matsumoto, "Experiments of One-Point Cold Fusion," *Fusion Technology*, vol 24, no 3, p 332 (1993).
4. T. Matsumoto, "Extraordinary Traces Produced during Pulsed Discharges in Water,"*Bulletin of the Faculty of Engineering*, Hokkaido Univ., no 175, p 73 - 86 (1995).
5. T. Matsumoto, "Observation of Quad-Neutrons and Gravity Decay During Cold Fusion," *Fusion Technology*, vol 19, no 4, p 2125 (1991).
6. T. Matsumoto, "Observation of Stars Produced During Cold Fusion," *Fusion Technology*, vol 22, p 518 (1992).
7. T. Matsumoto, "Experiments of Underwater Spark Discharges with Pinched Titanium Electrodes," to be published.
8. G. Elgey, The Mysterious Ball-Lightning, Japanese edition by Maruzen Co., Ltd., (c1990).
9. S. Silver, "Ball-Lightning," *Naturwissenschaften*, vol 67, p 332 (1980).

APPENDIX: **Feasible Schemes of Nuclear Transmutation**

Feasible schemes of the nuclear transmutation are discussed here by the Nattoh Model. The model predicted that a hydrogen-cluster is formed on the surface of the electrodes. Since the nuclear reactions take place under the multi-body interaction of the cluster constituents such as electrons, protons, oxygens and the heavy nuclei of the electrolyte and the host metals, there are various kinds of feasible schemes for the nuclear transmutation. The different kinds of nuclei produced by the nuclear transmutation depend on the applied voltage or the current density. As the voltage is increased, the higher order reactions could be enhanced. In this appendix, however, only the principal reactions will be considered here, taking an example of the iron electrode and the potassium electrolyte. The higher order reactions are straight forward.

A. Iron electrode

Natural iron contains four stable isotopes: ^{54}Fe (5.84%), ^{56}Fe (91.68 %), ^{57}Fe (2.17 %) and ^{58}Fe (0.3/%). The capture of an electron is not so effective for the nuclear transmutation of iron. Only the lightest isotope ^{54}Fe can be transformed by capturing an electron as follows:

$$^{54}Fe + e \rightarrow {}^{54}Mn \xrightarrow[EC]{313d} {}^{54}Cr(st) \tag{1}$$

The other isotopes of iron cannot be transmuted by capturing an electron because the products of ^{56}Mn, ^{57}Mn and ^{58}Mn rapidly undergo the beta decay to return back to the original nuclei.

When the iron isotopes capture a proton, new elements and different iron isotopes can be produced,

$$^{54}Fe + p \rightarrow {}^{55}Co \xrightarrow[EC]{17.5\,h} {}^{55}Fe \xrightarrow[EC]{2.7y} {}^{55}Mn(st) \tag{2}$$

$$^{56}Fe + p \rightarrow {}^{57}Co \xrightarrow[EC]{271d} {}^{57}Fe(st) \tag{3}$$

$$^{57}Fe + p \rightarrow {}^{58}Co \xrightarrow[EC/\beta^+]{70.8d} {}^{58}Fe(st) \tag{4}$$

$$^{58}\mathrm{Fe} + \mathrm{p} \rightarrow {}^{59}\mathrm{Co}\ (\mathrm{st}) \tag{5}$$

where EC and β^+ indicate the capture of an electron and the emission of a positron, respectively. The half-life of EC or β^+ in the itonic state should be drastically shortened, because the electrons of the itonic state distribute very closely to the nucleus. Through Eqs. (3) and (4), the isotope ratio of the iron element should deviate from the natural value. Furthermore, the iron isotopes can fuse each other and heavy elements such as cadmium can be produced, for example,

$$^{54}Fe + {}^{54}Fe \rightarrow {}^{108}Te \dashrightarrow {}^{108}Sb \dashrightarrow {}^{108}Sn \xrightarrow[EC]{10m} {}^{108}In \xrightarrow[EC/\beta^+]{40m/58m} {}^{108}Cd(st) \tag{6}$$

$$^{54}Fe + {}^{56}Fe \rightarrow {}^{110}Te \dashrightarrow {}^{110}Sb \dashrightarrow {}^{110}Sn \xrightarrow[EC]{4.2h} {}^{110}In \xrightarrow[EC/\beta^+]{69m/5h} {}^{110}Cd(st) \tag{7}$$

$$^{56}Fe + {}^{56}Fe \rightarrow {}^{112}Te \dashrightarrow {}^{112}Sb \xrightarrow[EC/\beta^+]{54s} {}^{112}Sn(st) \tag{8}$$

B. Potassium Electrolyte

Natural potassium consists of three isotopes of ^{39}K (93.2 %), ^{40}K (0.01%) and ^{41}K (6.7 %). The feasible schemes can be derived similarly as for iron.

For the capture of one electron,

$$^{40}K + e \rightarrow {}^{40}Ar\ (st) \tag{9}$$

where ^{39}K and ^{41}K cannot transmute by the electron capture.

For the capture of one proton, the calcium element can be produced as follows,

$$^{39}K + p \rightarrow {}^{40}Ca\ (st) \tag{10}$$

$$^{40}K + p \rightarrow {}^{41}Ca \xrightarrow[EC]{10^5 y} {}^{41}K\ (st) \tag{11}$$

$$^{41}K + p \rightarrow {}^{42}Ca\ (st) \tag{12}$$

It should be emphasized that during the nuclear transmutation in the hydrogen-clusters, neither energetic radiation nor activities could be generated. Even if the nuclei fuse each other to form an excited compound nucleus, the exciting energy could be transferred to the vibrational motion of the itonic mesh. Therefore, the nucleus could go to the ground state without emitting radiation. When the itonic mesh breaks up, however, the excited nucleus could emit high energy radiations as in the normal manner, and the activity also could somewhat persist.

Editor's Comments: This paper was not submitted for peer-review, however, the experimental data is timely and is an excellent addition to the papers published in this journal. See especially the paper by Jin et al., and the review paper by Bhadkamkar et al. in this issue, and the papers by Bass et al., Shoulders et al., and Fox et al. in the Fall 1996 issue of this journal. The adequacy of the Nattoh model is left for the future evaluation by peers. The author and the editor will welcome comments on both the experimental work and the author's Nattoh model.